



A Modification to Time-Series Coregistration for Sentinel-1 TOPS Data

Xin Tian, Zhang-Feng Ma , *Student Member, IEEE*, and Mi Jiang , *Senior Member, IEEE*

Abstract—Very high requirement of co-registration accuracy better than 0.001 pixels for Sentinel-1 TOPS (Terrain Observation by Progressive Scan) mode presents a great challenge for application of SAR (synthetic aperture radar) interferometry in Earth Observation. The state-of-the-art techniques have demonstrated that the low coherence scenarios and abrupt loss of coherence between two arbitrary acquisitions are main sources of error to degrade the performance of TOPS time-series co-registration. In this paper, we present a modification to overcome both limitations through the coherence enhancement. The motive behind this is to improve the quality of observations before co-registration and meanwhile avoiding the coherence loss caused by fast decorrelation. To this end, principal components analysis based spatio-temporal filtering is first used to remove the artifacts in burst interferograms over strong noise areas. Rather than heuristically choosing a sub-set of interferograms as a small baseline technique does, we use Dijkstra's shortest path algorithm under graph theory framework to maximize the coherence of a sub-set interferograms. The performance of presented method against the state-of-the-art techniques is fully evaluated by synthetic data and a Sentinel-1A stack over a low coherence scene in Indonesia. Comprehensive comparisons demonstrate 9%–17% uncertainty reduction of time-series co-registration when applying our method.

Index Terms—Coherence, coregistration, Sentinel-1, synthetic aperture radar (SAR), terrain observation by progressive scan (TOPS).

I. INTRODUCTION

THE Sentinel-1 satellite constellation has proven its capabilities in geodetic applications of synthetic aperture radar (SAR) by the advantages of the short revisit cycle (6 days for the combination of A and B) and the extensive coverage under the Interferometric Wide swath mode (IW). Terrain Observations by Progressive Scans (TOPS) [1], [2], the default SAR imaging mode of IW, can capture three sub-swaths with a width of 250 kilometers and achieve the entire antenna pattern of each observed target on Earth. Notably, the antenna beam of Sentinel-1

keeps electronically steering in each burst of three swaths (see Fig. 1) under TOPS mode. However, the introduced azimuth-independent Doppler centroid difference between consecutive bursts, which can be several times larger than pulse repetition frequency (PRF), presents a great challenge for TOPS image co-registration. Theoretically, a co-registration accuracy up to 0.001 pixels is required to remove the phase inconsistency of 3 degrees for orbital error of 5cm in the along-track direction [3]. Such high accuracy can be generally achieved by a two-step strategy: (1) coarse geometrical co-registration [4] based on external Digital Elevation Model (DEM) and precise orbital information; (2) fine co-registration using Enhanced Spectral Diversity (ESD) technique.

Suppose that ionospheric effect and azimuth deformation can be ignored, errors of co-registration after geometrical co-registration is primarily relevant to the orbital uncertainty, timing error of SAR instrument and accuracy of DEM [5]. These errors can contribute to a constant azimuth shift, which give rise to a phase jump between consecutive bursts in the differential interferograms.

ESD technique is an effective method to remove constant azimuth shift. Prats-Iraola *et al.* [3] compared the results of ESD with Spectral Diversity [6] and validated the better performance of ESD for TerraSAR-X TOPS data. Fattahi *et al.* [5] and Yague-Martinez *et al.* [7] introduced the principles of ESD in the context of Sentinel-1 mission. Like the split-band interferometric technique presented by Bamler and Eineder [8], ESD takes advantage of the interferometric phase difference between upper band and lower band (8% of each burst image size) to estimate the azimuth shift. Thus, the accuracy relies on the interferometric coherence [9]. When time-series images are available, temporal decorrelation is one of the primary sources of error to degrade the ESD performance. The state-of-the-art techniques dedicate to improving the coherence by choosing pairs with better coherence, coherent targets selection and phase optimization [5], [7], [9]. For example, Fattahi *et al.* proposed a network ESD approach (NESD) to reduce the impact of temporal decorrelation on mis-registration time-series. Similar with small baseline sub-set (SBAS), a sequential network that connects adjacent acquisitions within a time interval was used based on the exponential decorrelation model [10]. However, the assumption cannot be held over fast decorrelation scenarios or for the pairs suffering from abrupt loss of coherence due to climate conditions (e.g., snow and precipitation). As an alternative, MST-ESD [9] can overcome such abrupt coherence loss through constructing a minimum spanning tree (MST) and accurate coherence

Manuscript received February 17, 2020; revised March 15, 2020; accepted March 28, 2020. Date of publication April 17, 2020; date of current version May 1, 2020. This work was supported in part by the National Natural Science Foundation of China under Grant 41801244 and Grant 41774003, in part by the Natural Science Foundation of Jiangsu Province under Grant BK20171432, and in part by the ESA-MOST Dragon 4 project under Grant 32248_2. (*Corresponding author: Mi Jiang.*)

Xin Tian is with School of Transportation, Southeast University, Nanjing 211189, China (e-mail: tianxin@seu.edu.cn).

Zhang-Feng Ma is with School of Earth Sciences and Engineering, Hohai University, Nanjing 211100, China (e-mail: jspcmazhangfeng@hhu.edu.cn).

Mi Jiang is with State Key Laboratory of Hydrology-Water Resources and Hydraulic Engineering, Hohai University, Nanjing 210098, China, and also with the School of Earth Sciences and Engineering, Hohai University, Nanjing 211100, China (e-mail: mijiang@hhu.edu.cn).

Digital Object Identifier 10.1109/JSTARS.2020.2985503

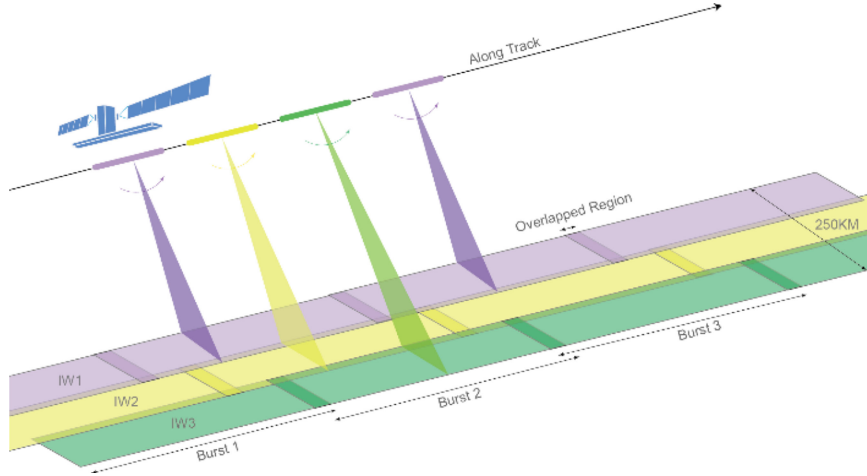


Fig. 1. Description of TOPS imaging geometry for Sentinel-1 satellite mission.

estimation. However, the reduction of observations may lead to error propagation during the least-squares adjustment. Some studies also deployed phase filtering to enhance the phase signal-to-noise ratio (SNR) at the cost of high computational burden or artifacts caused by spatial average over strong noise areas.

In sum, despite many successful applications reported in the state-of-the-art techniques, a number of these works have recognized that it is very difficult to ensure reliable estimation on ESD and therefore accurate time-series co-registration over low coherence scenarios. This article aims to solve this problem by phase optimization and Graph theory. First, we employ principal components analysis (PCA) along temporal dimension to optimize phase series in the overlap area between the consecutive bursts. This method will enhance phase SNR without giving rise to artifacts over strong noise areas. Second, different with previous studies that heuristically choosing a sub-set of interferograms as SBAS technique does, we use Dijkstra's shortest path algorithm to maximize the coherence of a sub-set interferograms and simultaneously persevering temporal network consistency. We will demonstrate that the redundant observations, together with high phase SNR, are essential for robust azimuth shift estimation.

The rest of article is organized as follows. Section II briefly reviews the ESD technique. Section III describes the rationality of our algorithm. The effectiveness of the presented method is fully evaluated by synthetic and real data sets in Section IV. Finally, conclusions is drawn in Section V.

II. BRIEF REVIEW TO ESD TECHNIQUE

ESD technique utilizes interferometric phase difference over the overlap regions to estimate the azimuth mis-registration error. The overlap regions locate at consecutive bursts in one subswath or adjacent bursts of neighboring subswaths (see Fig. 1). Considering high spectral separation Δf_{ovl} between consecutive bursts, the small fluctuation of azimuth mis-registration time Δt can give rise to an large variation of interferometric phase

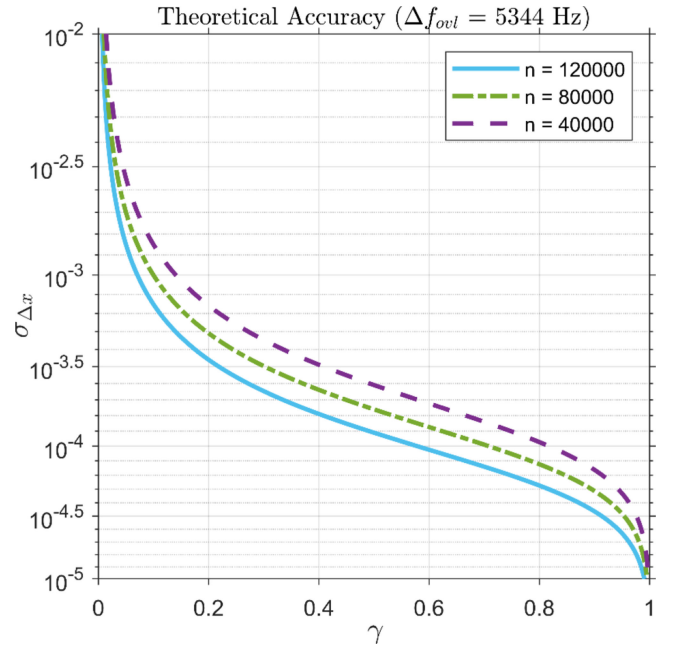


Fig. 2. Theoretical accuracy of the constant misregistration estimated by ESD within an overlap region containing 120 000, 80 000, and 40 000 coherent pixels, respectively.

difference ϕ_{ESD} ,

$$\phi_{ESD} = 2\pi\Delta f_{ovl}\Delta t \quad (1)$$

where $\Delta f_{ovl} \approx 5000$ Hz for Sentinel-1 TOPS mode [2]. The ESD phase ϕ_{ESD} of each pixel is generally estimated by differentiating burst interferograms in the overlap region [5], [9],

$$\phi_{ESD,p} = \angle((m_{i,p} \cdot s_{i,p}^*) \cdot (m_{i+1,p} \cdot s_{i+1,p}^*)^*) \quad (2)$$

where $m_{i,p}$ and $s_{i,p}$ represent the single look complex (SLC) image of i th master and slave bursts at spatial location p respectively. The superscript $*$ denotes complex conjugation operator and $m_{i,p} \cdot s_{i,p}^*$ indicates the burst interferogram.

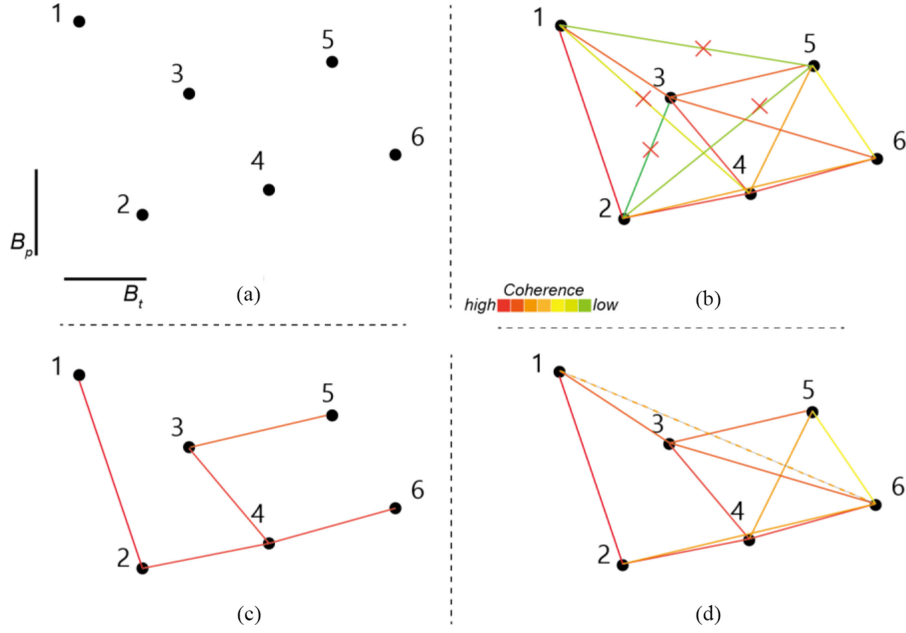


Fig. 3. Description of different temporal networks in the temporal (B_p)/perpendicular (B_t) baseline plane. (a) Distribution of TOPS image. (b) SBAS sub-set. (c) MST graph. (d) Dijkstra graph.

Theoretically, when precise or restituted orbits are provided, the ambiguity band is already solved after the geometric coregistration [7]. Thus, the ESD phase $\phi_{\text{ESD},p}$ of each pixel can be estimated from the wrapped phase histogram by a simple periodogram,

$$\hat{\Delta t} = \underset{\Delta t}{\operatorname{argmax}} \left\{ - \left| \sum_p e^{j(\phi_{\text{ESD},p} - 2\pi \Delta f_{\text{ovl}} \Delta t)} \right| \right\} \quad (3)$$

The solution space search is generally used to find optimal Δt . The spectral separation Δf_{ovl} is estimated from imaging geometry [3], [5], [9].

The azimuth shift Δx corresponding to ϕ_{ESD} is then calculated by

$$\Delta x = \frac{\Delta t}{\tau} = \frac{\phi_{\text{ESD}}}{2\pi \Delta f_{\text{ovl}} \tau} \quad (4)$$

where τ is the azimuth line time interval. Under the assumption that the same degree of noise exists over the overlap area in both burst interferograms, the estimate accuracy of the azimuth shift Δx can be evaluated by the phase noise standard deviation σ_ϕ [5], [9], [11],

$$\sigma_{\Delta x} = \frac{\sqrt{2}\sigma_\phi}{2\pi \Delta f_{\text{ovl}} \tau} \quad (5)$$

Consider the Cramér-Rao bound in the estimation of the co-registration error [8], the relationship between accuracy $\sigma_{\Delta x}$ and coherence γ can be expressed as,

$$\sigma_{\Delta x} = \frac{1}{2\sqrt{n}\pi \Delta f_{\text{ovl}} \tau} \frac{\sqrt{1-\gamma^2}}{\gamma} \quad (6)$$

where n is the sample size used to average.

III. METHODOLOGY

As shown in Fig. 2, the estimate accuracy of azimuth shift depends on sample size and coherence. This can be realized by the following two-step algorithm: 1) SNR enhancement through PCA and 2) Selection of redundant pairs with the best coherence through Dijkstra algorithm.

A. SNR Enhancement for Interferometric Phase

The mathematical formulation of optimum phase vector with respect to common master image $\hat{\theta}$ at each spatial location can be written as [12],

$$\hat{\theta} = \underset{\theta}{\operatorname{argmax}} \left\{ \theta^H \hat{\Sigma} \theta \right\} \quad (7)$$

where superscript H denotes the conjugate transpose. The quadratic form in (7) refers to a nonlinear optimization problem. According to the spectral theorem, this maximization can be realized by the Rayleigh quotient for Hermitian matrix $\hat{\Sigma}$, i.e., $\hat{\theta}$ corresponds to the eigenvector of the highest eigenvalue. Thus, we can optimize phase series by eigenvalue decomposition of $\hat{\Sigma}$, which is the sample covariance matrix estimated from a maximum likelihood estimator [13], [14],

$$\hat{\Sigma} = \frac{\mathbf{g}\mathbf{g}^H}{\sqrt{\|\mathbf{g}\|^2 (\|\mathbf{g}\|^2)^T}} \quad (8)$$

where matrix $\mathbf{g} \in \mathbb{C}^{N \times l}$ stands for l spatial pixels in N SLC images under a complex (circular) multivariate Gaussian model. Generally, l spatial pixels of each SLC image in a neighborhood should be homogeneous, i.e., the sample originates from the same distribution. Otherwise, the estimate of covariance matrix is biased. To mitigate heterogeneity and remove the bias of

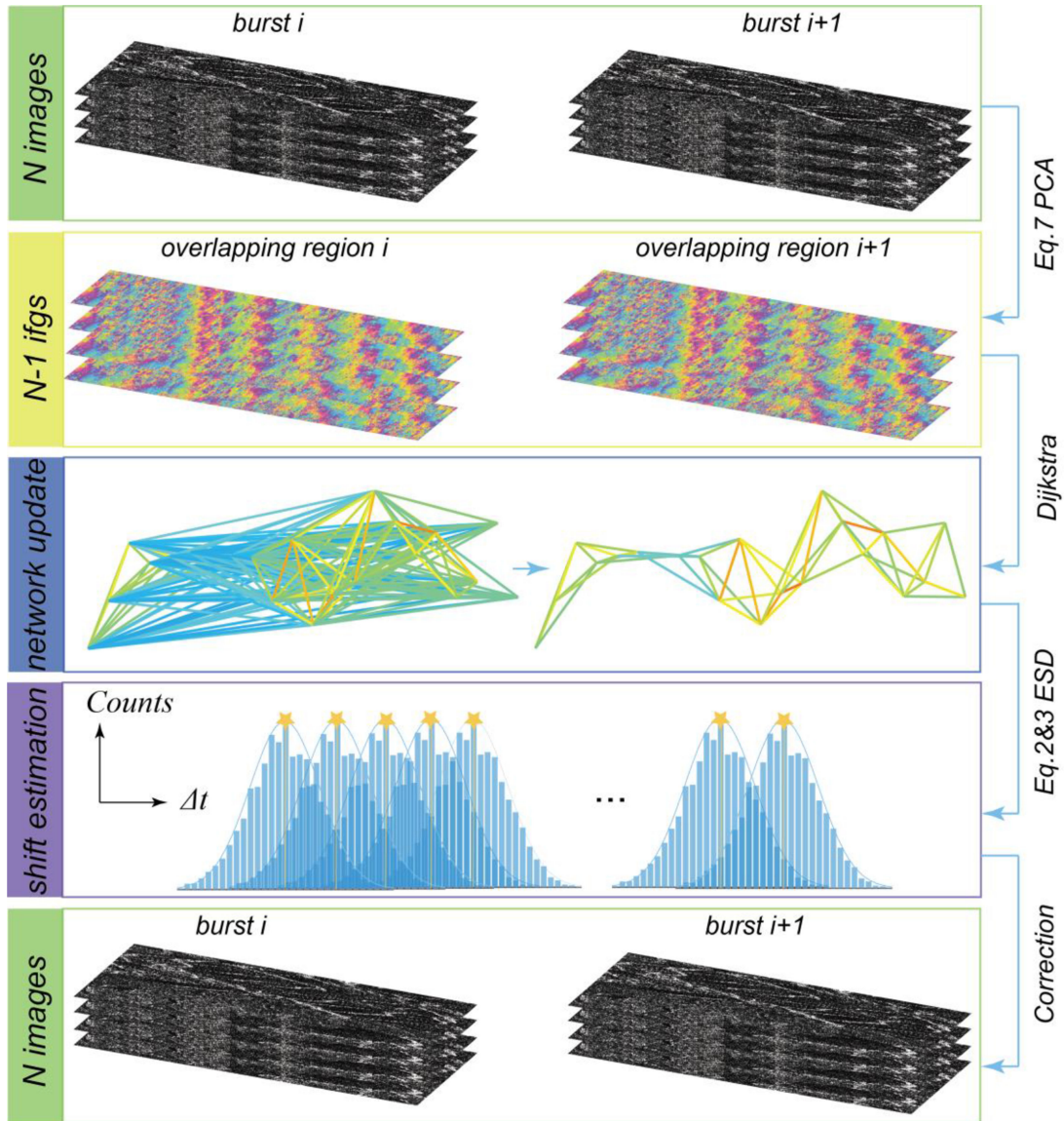


Fig. 4. Schematic concept of presented method (MESD) for Sentinel-1 TOPS time-series data co-registration.

sample covariance matrix, we employ FaSHPS Toolbox presented in [14]–[16], which is a highly efficient algorithm to select homogeneous neighbors using confidence interval for each spatial pixel in a neighborhood.

Once the covariance matrix is estimated, we use N dimensional subspaces decomposed by PCA to represent respective scattering mechanism [12]. Since the maximum eigenvector can provide the best mathematical approximation of covariance matrix in Frobenius norm [12], we only analyze the first eigenvector associated with the dominant scatter property. It is worth noting that the single scattering decomposition in this paper is a compromise between the computational efficiency and the loss of multiple scatter mechanism. After PCA analysis, the ESD phase between two arbitrary acquisitions can be re-calculated by (2). The performance gain of ESD phase estimation after introducing PCA is analyzed in Section IV.

B. Selection of Redundant Pairs With Best Coherence

In TOPS time-series co-registration, the azimuth shifts of time-series images can be retrieved from a temporal network in temporal/perpendicular baseline plane [see Fig. 3(a)]. Generally, the redundant edges with better quality will improve the estimate accuracy during the least-squares adjustment. Since ESD estimator is not likely to correct phase jumps for low coherence pairs, the error propagation in SBAS network in Fig. 3(b) degrades the performance of co-registration. As an alternative, MST in Fig. 3(c) can avoid error propagation by maximizing coherence. It is easy to see, however, MST has no redundant edges. Thus, more sophisticated approach, that increases the pairs with better coherence is required. This can be realized by means of Dijkstra's algorithm under graph theory.

Starting from a weighted, undirected graph $G = (V, E)$ with weight function $w : E \rightarrow \mathbb{R}^+$, where $V = [v_1, v_2, \dots, v_N]$ is

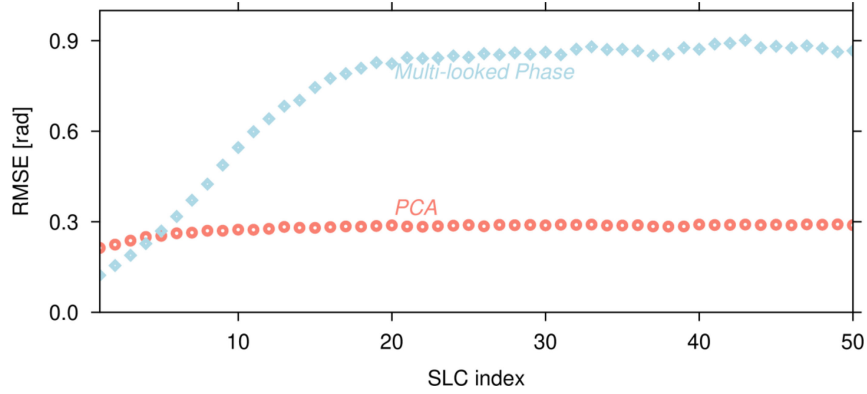


Fig. 5. Root mean square error of phase optimization for time-series wrapped phase after 10 000 times Monte Carlo simulation. The light blue and salmon makers denote the RMSE of multilooked and optimum phase, respectively.

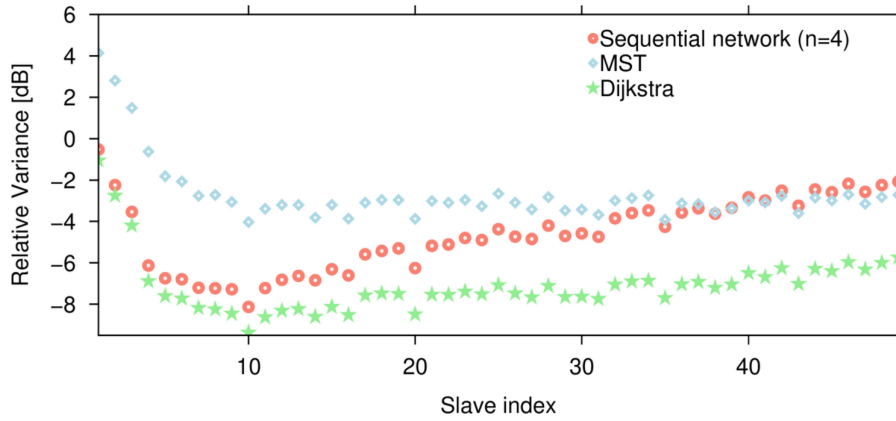


Fig. 6. Relative variance of ESD estimation using different temporal networks with respect to the single master ESD estimation. The salmon circles represent sequential network used in NESD; the light blue diamonds denote MST network used in MSTESD. The light green pentagrams are Dijkstra network used in MESD.

vertex in index order and E is a set of all possible edges, the objective of Dijkstra shortest path algorithm is to find a path from each source v_i to terminal v_j having the minimum weight. Dijkstra proceeds by relaxation, in which approximations to the correct distance calculated by weight are replaced by better ones until they eventually reach the solution [17]. It is asymptotically the fastest known single-source shortest-path algorithm for unbounded non-negative weights.

To our case, the vertex set V is composed of TOPS acquisitions in chronological order with size N . E is a edge set of $N(N-1)/2$ interferometric pairs between two arbitrary acquisitions. Using covariance matrix estimator (8), the coherence of all pairs is known. Therefore, we can define the weight as,

$$w_{i,j} = \frac{1}{\gamma_{i,j} - \varepsilon}, \text{ where } \gamma_{i,j} \in [0, 1] \text{ and } \varepsilon < \gamma_{i,j} \quad (9)$$

which stretches the contrast between low and high coherence value. Here $\gamma_{i,j} = \{|\hat{\Sigma}|\}_{i,j}$ denotes coherence which is the element of the magnitude of covariance matrix at the i th row and the j th column. ε is a compensation term to eliminate the impact of the coherence bias on weighting. After defining an initial SBAS

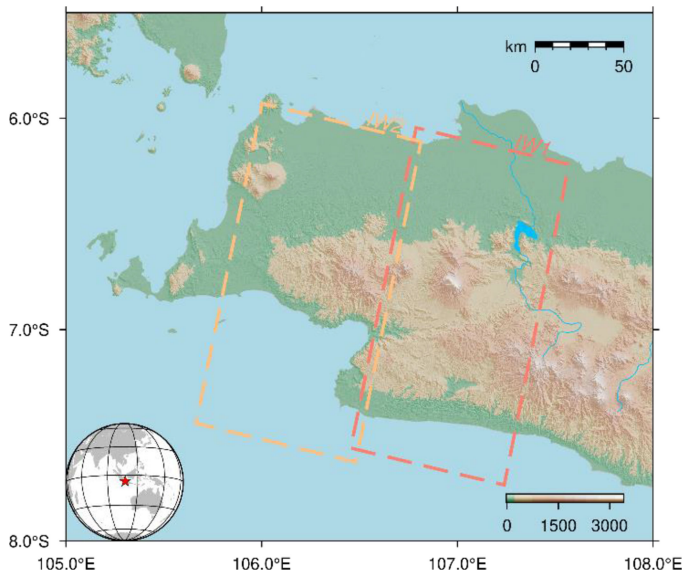


Fig. 7. Footprint of Sentinel-1 TOPS data covering an area in Indonesia (Track 47).

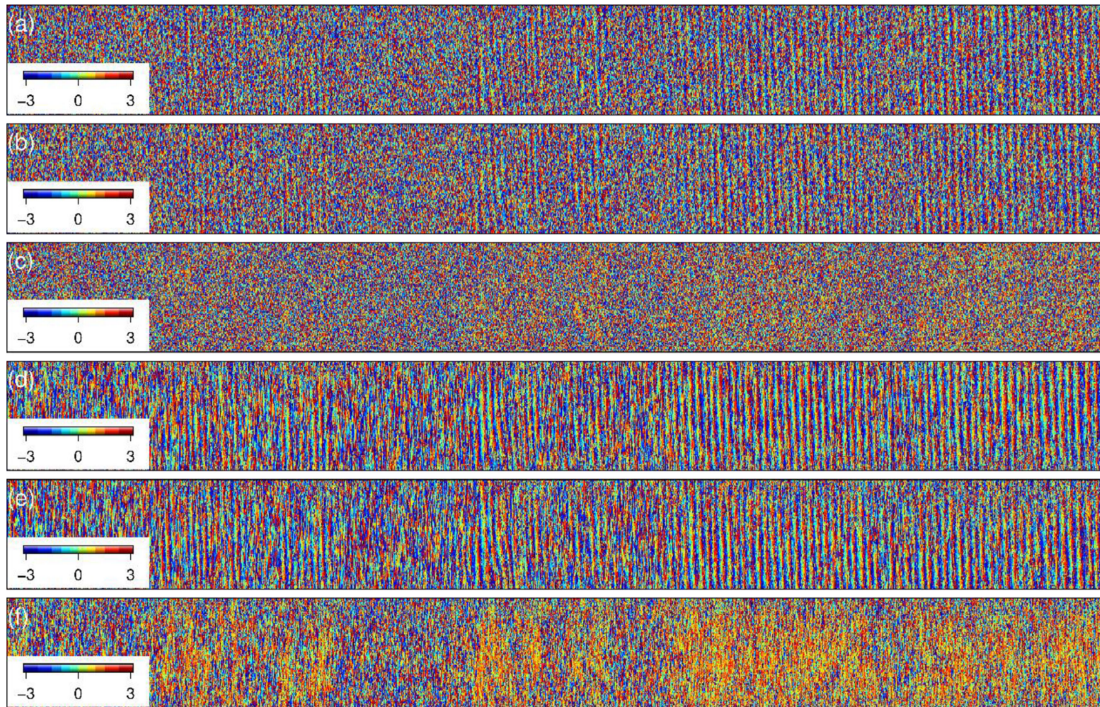


Fig. 8. Interferograms and ESD phases of the first overlap region in IW1 (20180719-20181128). (a) and (b) represent the burst interferogram of Burst1 and Burst2, respectively. (d) and (e) correspond to filtered burst interferograms after PCA analysis. (c) and (f) are ESD phase before and after phase optimization.

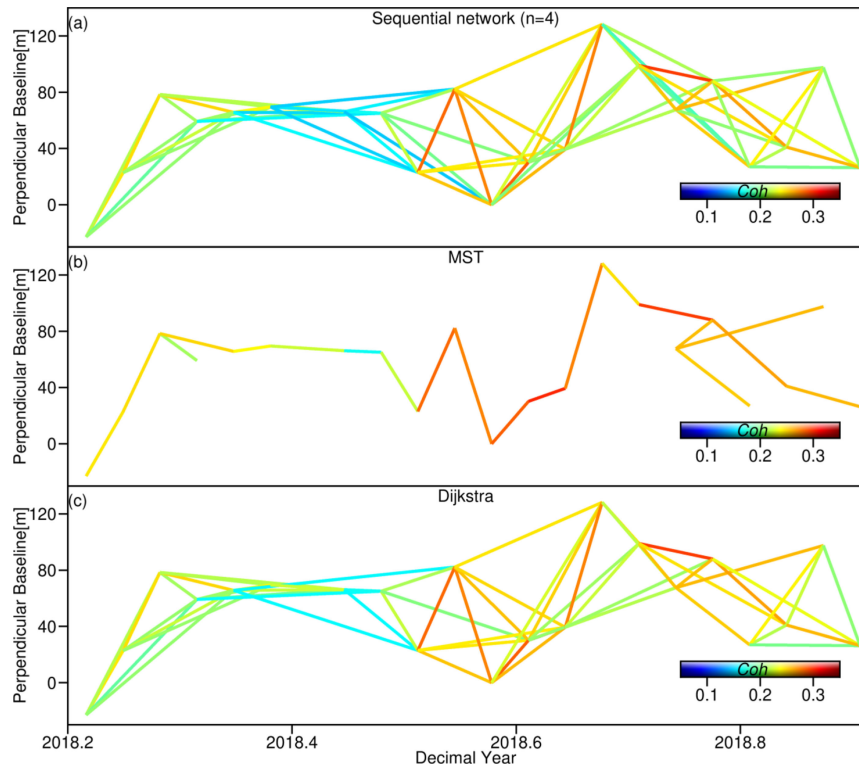


Fig. 9. Temporal network of Sentinel-1 dataset. (a) Sequential network with 4 degree used in ESD. (b) MST network used in MSTESD. (c) Dijkstra network used in MESD.

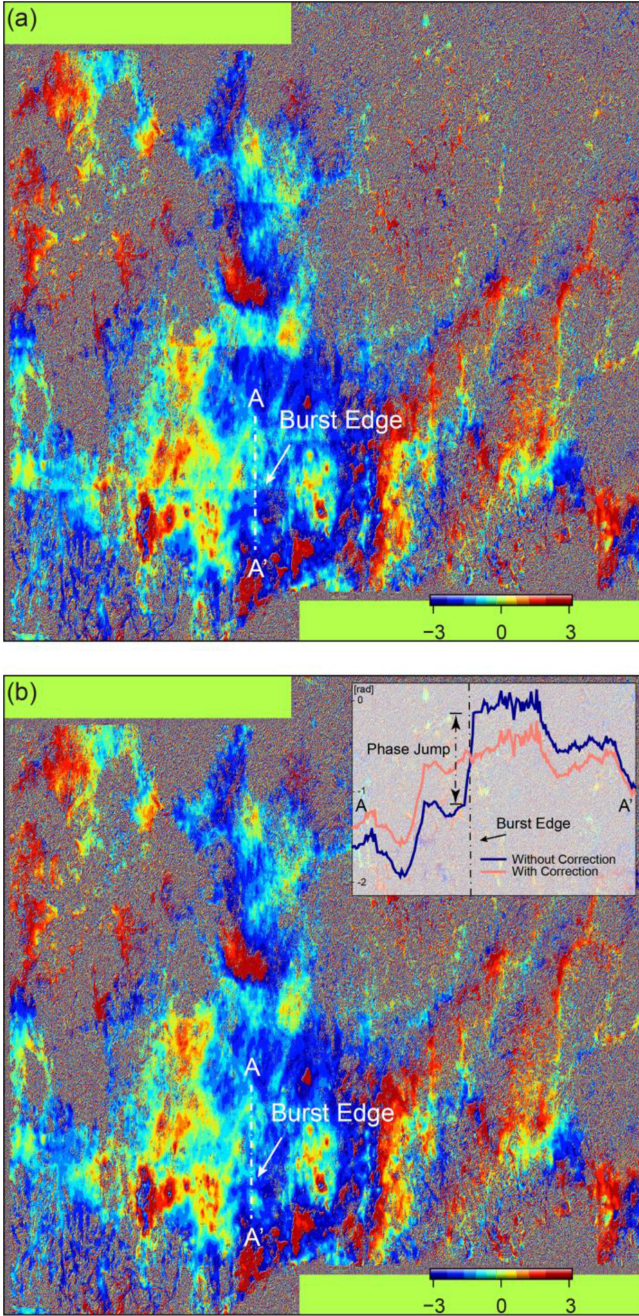


Fig. 10. Interferograms of 20180719 (YYYYMMDD)-20181128 (YYYYMMDD). (a) Interferogram without misregistration correction. (b) Interferogram corrected from MESD; all interferograms have been filtered for visual interpretation; the transect AA' covering the edge of consecutive bursts in (a) is shown in (b), and the phase jump can be clearly observed.

sub-set in which the temporal and perpendicular baseline less than a threshold, we use (9) to find the shortest path for each pair (v_i, v_j) in the sub-set through Dijkstra's algorithm until last pair in the sub-set has been updated.

The primary advantage of the presented method is that Dijkstra not only finds pairs with better coherence from the whole interferometric configurations, but also ensures the connection for vertices. This behavior avoids isolated sub-sets which lead

to rank deficiency during the inversion. In Fig. 3(d), one can see the new temporal network adds a good edge (dash line) and remove the poor edges (labelled as a cross) in a SBAS network in Fig. 3(b). Compared with MST graph in Fig. 3(c), Dijkstra can provide more redundant observations.

C. Modified ESD Algorithm

Fig. 4 presents a schematic concept of the modified ESD algorithm for TOPS time-series data co-registration. After geometrical co-registration using DEM and Sentinels Precise Orbit Determination (POD), the phase series of upper (i th) and lower ($i+1$ th) bursts series are first optimized using (7) respectively. The topographical phase component should be compensated by DEM. Then $N(N-1)/2$ coherence can be obtained by (8). Because coherence of all pairs has been estimated during phase optimization, it is not necessary to re-calculate coherence again. Once the sub-set of interferograms with best coherence is selected by Dijkstra's algorithm, the ESD phase series can be calculated by differentiating optimum phase using (2), followed by azimuth shift estimation using (3). A weighted least square adjustment is finally implemented to retrieve azimuth shifts with respect to a common reference. The presented method is hereafter referred to as MESD in the following analysis.

IV. RESULTS AND ANALYSIS

In this section, the performance of developed MESD method is fully evaluated and compared against the state-of-the-art techniques including NESD and MSTESD, using synthetic and real data.

A. Synthetic Data

The goal of this section is to evaluate the effect of phase optimization and its impact on ESD phase estimation. The simulation was implemented as follows [7], [15], [18], [19]:

- 1) An exponential decorrelation model was deployed to simulate true covariance matrix in (7). The decorrelation rate with a constant period of 27 days was set. The short-term and long-term coherence was set to 0.6 and 0.1 respectively to simulate low coherence scenarios.
- 2) $N = 50$ SLC single-look images with $l = 100$ homogeneous pixels were simulated by true covariance matrix and a complex Gaussian matrix with zero mean and 0.5 variance. The time interval between two consecutive acquisitions was set to 12 days which is same with Sentinel-1A satellite mission. To highlight the impact of stochastic noise on interferometric phase, no other component is added. 10 000 times Monte Carlo simulation were carried out and the Root Mean Square Error (RMSE) between the truth and estimate was counted.

During phase optimization, covariance matrix was first calculated using (8), followed by conventional multi-looking used in NESD and MSTESD and PCA analysis in (7) respectively. In Fig. 5, the RMSE of phase series after phase optimization is smaller than that using multi-looking for most SLC image series. The averaged RMSE for the whole series reduces from

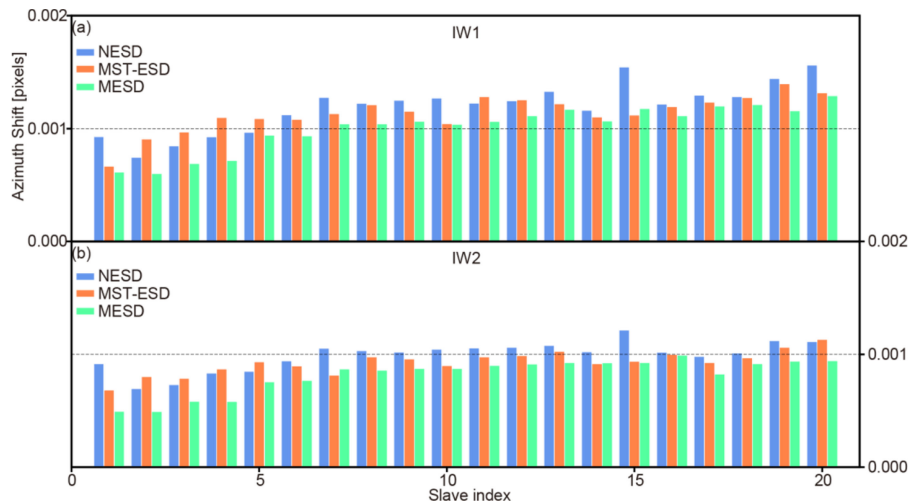


Fig. 11. Standard deviation of the azimuth misregistration residuals of Sentinel-1 TOPS series after 50 iterations.

~ 0.86 to ~ 0.29 rad. This result demonstrates PCA method has a significant effect on the improvement of the accuracy of interferometric phase series.

Next, we evaluated the impact of temporal network on azimuth co-registration. The Dijkstra network presented in Section III-B, MST network in MSTESD and sequential network with $n = 4$ in NESD have compared each other. We first randomly added coherence value between -0.1 and 0.3 into covariance matrix to simulate an abrupt loss of coherence. Then two stacks were simulated using the same covariance matrix. The azimuth shifts in the interval $[-0.02, 0.02]$ pixels were finally added randomly into a stack. To avoid the influence of phase and coherence estimators on co-registration, the estimators and weight used for least squares adjustment as well as parameters are same except temporal network.

Under each simulation, the azimuth shift of each slave image relative to a common master (the first image) was first calculated. Then sequential network, MST and Dijkstra's algorithm were applied. We implemented simulation 10 000 times and counted the relative variance of each method with respect to that from individual ESD estimation, and then transformed them into dB. The negative values imply a reduction of variance after the least-squares inversion. In Fig. 6, we can see that ESD using developed temporal network can obtain better co-registration accuracy. This is understandable because the network redundancy with better quality results in more robust ESD estimation during inversion. On the contrary, the decrease of network redundancy in MST degrades the performance of time-series co-registration, although it has the best observations quality. However, the increase of redundancy cannot ensure better estimate accuracy for the sequential network as the observations with low coherence lead to the error propagation.

B. Real Data

Two sub-swaths of 21 Sentinel-1A with TOPS mode acquired from February, 2018 to September, 2018 were processed. The

test site located in Indonesia is dominated by heavily vegetable land cover (see Fig. 7). The typical tropical rainforest climate with an average annual temperature of 25°C and annual rainfall of about 2000 mm makes the scene appropriate for validation at low coherence condition.

Fig. 8 shows upper and lower burst interferograms without de-fringing in the first overlapping regions of IW1. One can see fringe patterns over strong noise areas can be partly retrieved after phase optimization, showing the SNR enhancement of interferometric phase. By differentiating burst interferograms using (2), the quality of ESD phase in Fig. 8(f) is greatly improved than that in Fig. 8(c).

Fig. 9 presents the procedure of the selection of interferometric pairs. The sequential network in Fig. 9(a) still contains some edges with very low coherence. On the contrary, a sub-set selected from MST in Fig. 9(b) can preserve edges with high coherence at the cost of reduced redundancy. The presented method in Fig. 9(c) however, can remove bad edges in Fig. 9(a) and simultaneously preserving the network consistency that is missed in Fig. 9(b). The enhanced network can not only improve the computational efficiency but reduce error propagation caused by the bias of coherence estimator and artifacts in the burst interferograms.

After phase optimization and temporal network evolution, azimuth shifts of slave images can be inversed. Fig. 10 shows an interferometric pair between 20 180 719 and 20 181 128 before and after correction of shift. One can see that the phase jump along the transect of AA' in Fig. 10(a) has been corrected in Fig. 10(b) after applying MESD, confirming the effectiveness of presented method.

We further evaluated the co-registration accuracy for different ESD techniques. Quantitatively, we estimated azimuth shifts for $N-1$ pairs and carried out co-registration by means of resampled images after previous correction. We repeated this procedure 50 times under each method and each time counted the azimuth shift residuals. The closer the dispersion of residuals is to zero, the better the accuracy of co-registration. To illustrate

the performance at different coherence scenarios, swath1 with averaged coherence ~ 0.2 and swath2 with averaged coherence magnitude ~ 0.4 were tested respectively.

In Fig. 11, we calculated standard deviation (STD) for residuals of each slave image. Evidently, whatever the method is used, the co-registration accuracy degrades with the decrease of coherence. However, MESD is superior to NESD and MSTESD for most image series. In swath1, the averaged STD of residuals is 0.0012 pixels for NESD and 0.0011 pixels for MSTESD respectively. It decreases to 0.0010 pixels for MESD. In swath2 with better coherence, the STD decreases to 0.00098 pixels for NESD and 0.00092 pixels for MSTESD respectively. The MESD has a minimum STD up to 0.00081 pixels. In both cases, the empirical uncertainty reduction of 9%–17% validates the improved performance of presented method.

V. CONCLUSION

In this paper, we presented a modification for Sentinel-1 TOPS time-series co-registration over low coherence scenarios. The primary novelties lie in (1) using PCA analysis to enhance SNR of the phase series and simultaneously reducing artifacts caused by spatial smoothness over strong noise areas, and (2) employing a single source shortest path algorithm to refine temporal network instead of heuristically choosing a sub-set of interferograms as SBAS does. The former ensures more accurate estimation of ESD phase over low coherence scenarios, whereas the latter can avoid the adverse effect of abrupt loss of coherence on time-series co-registration. Using synthetic data and real Sentinel-1 TOPS stack in Indonesia, the advantage of presented method against state-of-the-art techniques has been fully validated. The results revealed that the MESD can reduce empirical uncertainty of 9%–17% compared to the NESD and MSTESD. We can conclude that the presented method outperforms state-of-the-art techniques over low coherence scenarios and can provide more robust co-registration products for geophysical applications.

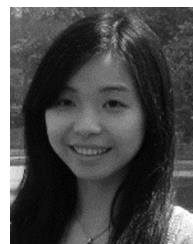
ACKNOWLEDGMENT

The Sentinel-1 data were provided by ESA/Copernicus. The figures in this paper were drawn by Generic Mapping Tools 6.0.0.

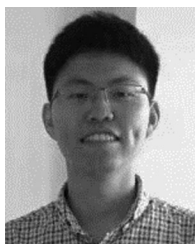
REFERENCES

- [1] F. De Zan and A. M. Guarnieri, "TOPSAR: Terrain observation by progressive scans," *IEEE Trans. Geosci. Remote Sens.*, vol. 44, no. 9, pp. 2352–2360, Sep. 2006.
- [2] R. Torres *et al.*, "GMES Sentinel-1 mission," *Remote Sens. Environ.*, vol. 120, pp. 9–24, 2012.
- [3] P. Prats-Iraola, R. Scheiber, L. Marotti, S. Wollstadt, and A. Reigber, "TOPS interferometry with TerraSAR-X," *IEEE Trans. Geosci. Remote Sens.*, vol. 50, no. 8, pp. 3179–3188, Aug. 2012.
- [4] E. Sansosti, P. Berardino, M. Manunta, F. Serafino, and G. Fornaro, "Geometrical SAR image registration," *IEEE Trans. Geosci. Remote Sens.*, vol. 44, no. 10, pp. 2861–2870, Oct. 2006.
- [5] H. Fattahi, P. Agram, and M. Simons, "A network-based enhanced spectral diversity approach for TOPS time-series analysis," *IEEE Trans. Geosci. Remote Sens.*, vol. 55, no. 2, pp. 777–786, Feb. 2016.

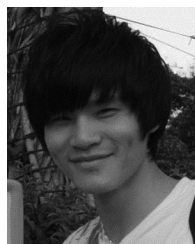
- [6] R. Scheiber and A. Moreira, "Coregistration of interferometric SAR images using spectral diversity," *IEEE Trans. Geosci. Remote Sens.*, vol. 38, no. 5, pp. 2179–2191, Sep. 2000.
- [7] N. Yague-Martinez, F. De Zan, and P. Prats-Iraola, "Coregistration of interferometric stacks of Sentinel-1 TOPS data," *IEEE Geosci. Remote Sens. Lett.*, vol. 14, no. 7, pp. 1002–1006, Jul. 2017.
- [8] R. Bamler and M. Eineder, "Accuracy of differential shift estimation by correlation and split-bandwidth interferometry for wideband and delta-k SAR systems," *IEEE Geosci. Remote Sens. Lett.*, vol. 2, no. 2, pp. 151–155, Apr. 2005.
- [9] Z. Ma, M. Jiang, Y. Zhao, R. Malhotra, and B. Yong, "Minimum spanning tree co-registration approach for time-series Sentinel-1 TOPS data," *IEEE J. Sel. Topics Appl. Earth Observ. Remote Sens.*, vol. 12, no. 8, pp. 3004–3013, Aug. 2019.
- [10] P. Berardino, G. Fornaro, R. Lanari, and E. Sansosti, "A new algorithm for surface deformation monitoring based on small baseline differential SAR interferograms," *IEEE Trans. Geosci. Remote Sens.*, vol. 40, no. 11, pp. 2375–2383, Nov. 2002.
- [11] A. M. Guarnieri and S. Tebaldini, "Hybrid Cramér–Rao bounds for crustal displacement field estimators in SAR interferometry," *IEEE Signal Process. Lett.*, vol. 14, no. 12, pp. 1012–1015, Dec. 2007.
- [12] G. Fornaro, S. Verde, D. Reale, and A. Pauciuolo, "CAESAR: An approach based on covariance matrix decomposition to improve multibaseline-multitemporal interferometric SAR processing," *IEEE Trans. Geosci. Remote Sens.*, vol. 53, no. 4, pp. 2050–2065, Apr. 2015.
- [13] Y. Wang and X. X. Zhu, "Robust estimators for multipass SAR interferometry," *IEEE Trans. Geosci. Remote Sens.*, vol. 54, no. 2, pp. 968–980, Feb. 2016.
- [14] M. Jiang *et al.*, "The potential of more accurate InSAR covariance matrix estimation for land cover mapping," *ISPRS J. Photogrammetry Remote Sens.*, vol. 126, pp. 120–128, 2017.
- [15] M. Jiang and A. M. Guarnieri, "Distributed scatterer interferometry with the refinement of spatiotemporal coherence," *IEEE Trans. Geosci. Remote Sens.*, to be published, doi: [10.1109/TGRS.2019.2960007](https://doi.org/10.1109/TGRS.2019.2960007).
- [16] M. Jiang, X. Ding, R. F. Hanssen, R. Malhotra, and L. Chang, "Fast statistically homogeneous pixel selection for covariance matrix estimation for multitemporal InSAR," *IEEE Trans. Geosci. Remote Sens.*, vol. 53, no. 3, pp. 1213–1224, Mar. 2015.
- [17] T. H. Cormen, C. E. Leiserson, R. L. Rivest, and C. Stein, *Introduction to Algorithms*. Cambridge, MA, USA: MIT Press, 2009.
- [18] H. Ansari, F. De Zan, and R. Bamler, "Efficient phase estimation for interferogram stacks," *IEEE Trans. Geosci. Remote Sens.*, vol. 56, no. 7, pp. 4109–4125, Jul. 2018.
- [19] H. Ansari, F. D. Zan, and R. Bamler, "Sequential estimator: Toward efficient InSAR time series analysis," *IEEE Trans. Geosci. Remote Sens.*, vol. 55, no. 10, pp. 5637–5652, Oct. 2017.



Xin Tian received the B.S. degree in geographic information system in 2005, and the Ph.D. degree in photogrammetry and remote sensing in 2013, both from Wuhan University, Wuhan, China. She was a joint Ph.D. student in environment and resource studies, University of Waterloo, Canada, during the period from Oct. 2008 to Feb. 2010. She is currently a Lecturer in Southeast University, Nanjing, China. Her research interests include SAR data processing, SAR interferometry and SAR applications such as surface displacements monitoring, land cover mapping and change detection. Dr. Tian serves as a Referee for *Geophysical Journal International*, the *IEEE Journal of Selected Topics in Applied Earth Observations and Remote Sensing*.



Zhang-Feng Ma (Student Member, IEEE) was born in Nantong, Jiangsu Province, China in 1995. He received the B.S. degree in geomatics from Nanjing University of Technology, Nanjing, China, and the Master's degree in geomatics engineering from Hohai University, Nanjing, China. Currently he is pursuing Ph.D degree in Hohai University. His research interests include interferometric synthetic aperture radar and its application for monitoring and modeling ground surface deformation.



Mi Jiang (Senior Member, IEEE) was born in Nanjing, China, in 1982. He received the B.S. degree in computational mathematics from the Nanjing University of Technology, Nanjing, China, the M.Sc. degree in radar remote sensing from the Central South University, Changsha, China and the Ph.D. degree from The Hong Kong Polytechnic University, Hong Kong, China. He is currently a Professor with the School of Earth Science and Engineering, Hohai University, Nanjing, China. His current research interests are in the field of statistical inference with emphasis on synthetic aperture radar processing.